Intercomparison of 3D turbulence parameterizations for dispersion models in complex terrain derived from a circulation model (*)

S. TRINI CASTELLI ([1]) and D. ANFOSSI ([2])
([1]) *Istituto di Fisica Generale, Università di Torino - Via Giuria 1, Torino, Italy*
([2]) *CNR, Istituto di Cosmogeofisica - Corso Fiume 4, Torino, Italy*

(ricevuto il 10 Gennaio 1996; revisionato il 19 Settembre 1996; approvato il 10 Ottobre 1996)

Summary. — A procedure for estimating 3D turbulent parameters from the outputs of a circulation model to be used as input of a random flight model for complex terrain dispersion simulation is presented. It is based on parameterization schemes for surface layer parameters and wind velocity standard deviation profiles available in the literature. The predictions of various schemes (two for surface layer quantities and three either for the PBL depth or standard deviation profiles) have been compared to observations carried out in the alpine region (south Switzerland) during the second TRANSALP campaign by three Doppler Sodar and two sonic anemometers.

PACS 92.60.Sz – Air quality and air pollution.
PACS 92.60.Fm – Boundary layer structure and processes.
PACS 01.30.Cc – Conference proceedings.

1. – Introduction

Correctly predicting the pollutant dispersion in complex terrain, where orography produces inhomogeneous fields of mean wind speed and turbulence, is of great importance. The spatial variations of wind velocity moments are to be taken into account and therefore the complete 3D structure of the turbulent flow must be considered: in these conditions Lagrangian particle models proved to be able to yield reliable simulations of atmospheric turbulent dispersion (see, for instance, papers [1-8]). Apart from the design of the dispersion model itself, the input 3D flow and turbulence fields are the key aspects of the turbulent dispersion modelling: the first ones are generally obtained by circulation or mass consistent models, whereas

(*) Paper presented at EUROMECH Colloquium 338 “Atmospheric Turbulence and Dispersion in Complex Terrain” and ERCOFTAC Workshop “Data on Turbulence and Dispersion in Complex Atmospheric Flows”, Bologna, 4-7 September 1995.

the second ones are derived from parameterizations based on both the available measurements and the circulation model outputs.

The aim of this paper is to present our parameterization scheme for 3D turbulence fields. This scheme constitutes the link between a flow model [9] and our dispersion particle model SPRAY [5], but it can be generalised and adapted to other models. It makes use of both the measured information (if any) and the output from the circulation model (3D wind velocity and potential temperature fields) to get the fields needed for the dispersion model by means of proper parameterizations. To prescribe the surface layer parameters (friction velocity u_*, Monin-Obukhov length L, sensible heat flux h_0 and the flux temperature θ_*) two different methods are adopted: the meteorological pre-processor PBL-MET [10] and the Louis formulation [11]. To assign the values of 3D vertical profiles of standard deviation and Lagrangian time scales of the three wind velocity fluctuations, expressed as functions of the above surface layer parameters, three schemes are selected, suggested by Hanna [12], Rodean [13] and Pielke's team [14, 15], respectively.

The results obtained using the different options of our scheme are compared to each other and to some measurements from the second TRANSALP meteorological and tracer campaign. This was carried out on September 29th, 1990 in the Ticino river valley, southern Switzerland. Its purpose was the study of air masses and pollutant transport through the Alps [16]. The measurements considered throughout this paper were performed by means of Doppler Sodars, sonic anemometers and temperature soundings in a rather complex area during typical valley breeze condition. The wind and temperature fields employed here as input were obtained by Martilli and Graziani [17] by RAMS.

The quality and accuracy of comparison results presented in this paper may be of some interest since the surface layer and Planetary Boundary Layer (PBL) relationships that are considered in the above schemes have been derived from horizontally uniform, flat terrain measurements. Little is known about the accuracy of these parameterizations in complex terrain. This is particularly true in the alpine area, where flow conditions are extremely varying (both in the horizontal and in the vertical direction) due to the presence of main and lateral valleys, ridges, air stagnation regions in the lee of obstacles, separation of the flow, differentially heated valley walls. Furthermore, many of these phenomena are not resolvable on the grid spacing of input circulation model.

The various turbulence parameterizations are introduced in sect. **2**. TRANSALP 1990 campaign and related meteorological measurements are presented in sect. **3**. Then a brief outline of flow fields simulated by RAMS for the same campaign [17] and used in this work as input to the parameterization scheme appears in sect. **4**. Finally, sect. **5** deals with the results of the present analysis.

2. – Turbulence parameterization scheme

The physical basis for computing surface parameters and turbulence fields, needed for the dispersion model, is provided by parameterizations of the PBL structure, including its interaction with the ground. Here the parameterization of the meteorological quantities has been developed in two stages. In the first one the surface layer parameters, useful to estimate the temporal evolution of PBL structure, are computed; in the second one, the vertical profiles of turbulence field are estimated.

In this work the following gridded fields are supposed to be known: three wind components and potential temperature profiles, roughness z_0 and topography. Diffusion coefficients may also be considered.

2˙1. *Surface layer parameters.* – The first step of this stage consists in estimating the values of, u_*, L, θ_* and, h_0, which are necessary to compute the PBL depth h and some of the PBL quantities. Two different methods are considered: the first one (SL1) makes use of the meteorological pre-processor PBL-MET [10] and the second one (SL2) employs Louis relationships [11]. Both methods are based on the Monin-Obukhov theory for the atmospheric surface layer.

Accounting for the stability functions proposed by Businger *et al.* [18] and Van Ulden and Holtslag [19], and making use of a single wind speed and a single temperature difference within the surface layer, SL1 yields an estimate of u_*, θ_*, and L by an iterative procedure. We remind that L is computed as

$$L = \frac{\overline{\theta} u_*^2}{gk\theta_*},$$

where g is the acceleration due to gravity, k is the von Karman constant and $\overline{\theta}$ is the mean potential temperature.

On the contrary SL2 avoids any iteration method. Defining the bulk Richardson number $\mathrm{Ri_B}$ as

$$\mathrm{Ri_B} = \frac{gz\,\Delta\theta}{\overline{\theta} U^2},$$

where $\Delta\theta$ is the potential temperature difference through the layer considered and U is the wind speed, it is possible [11] to write u_* and θ_* as functions of z/z_0 and $\mathrm{Ri_B}$:

$$u_*^2 = a^2 U^2 F_m\left(\frac{z}{z_0}, \mathrm{Ri_B}\right),$$

$$u_*\theta_* = \frac{a^2}{R} U \Delta\theta F_h\left(\frac{z}{z_0}, \mathrm{Ri_B}\right),$$

where $a^2 = k^2/(\ln(z/z_0))^2$ is the drag coefficient in neutral conditions and R is the ratio of the drag coefficients for momentum and heat in the neutral limit and is equal to 0.74 [18]. Keeping in mind that F may have different coefficients for momentum and heat, Louis [11] defined a common function and proposed

$$F = -\frac{b\,\mathrm{Ri_B}}{1 + c\,|Ru_B|^{1/2}}$$

in the unstable case ($\mathrm{Ri_B} < 0$), and

$$F = \frac{1}{(1 + b'\,\mathrm{Ri_B})^2}$$

in stable conditions ($\mathrm{Ri_B} > 0$). Imposing the first derivative of F to be continuous between the stable and the unstable conditions, he obtained $b = 2b' = 9.4$, while c was

found doing a dimensional analysis in the free convection limit: $c = C^* a^2 b (z/z_0)^{1/2}$, with $C^* = 7.4$ for momentum and $C^* = 5.3$ for heat fluxes.

Louis parameterization yields the profile of the diffusion coefficient as well:

$$K_m = l^2 \left| \frac{\Delta U}{\Delta z} \right| F(\mathrm{Ri}) \tag{1}$$

where Ri is the gradient Richardson number $\mathrm{Ri} = \frac{g \Delta z \Delta \theta}{\bar{\theta} (\Delta U)^2}$ and $l = \frac{kz}{1 + kz/\lambda}$ is the mixing length, λ being the asymptotic mixing length.

2˙2. PBL *height*. – To calculate the PBL depth h on the ground of the u_*, L and θ^* values above computed, three different methodologies are chosen. In the first one (PBL*h*1), following the simple model of the daytime PBL height proposed by Gryning and Batchvarova [20] and neglecting the spin-up term, it is possible to compute h solving the following differential equation:

$$\left[\frac{h^2}{(1 + 2A)\, h - 2BkI} \right] \frac{\mathrm{d}h}{\mathrm{d}t} = \frac{(\overline{w'\theta'})_s}{\gamma}, \tag{2a}$$

where $(\overline{w'\theta'})_s = h_0 / \varrho c_p$ and $A = 0.2$, $B = 2.5$; γ is the potential temperature gradient at dawn, $(\overline{w'\theta'})_s$ is the vertical kinematics heat flux at the surface, ϱ is the air density and c_p is the specific heat of dry air. The initialisation of the mixing height is based on the height of the turbulent stable boundary layer before convection starts. Some tests have also been made with the more general expression [21]

$$\left\{ \frac{h^2}{(1 + 2A)\, h - 2BkL} + \frac{c u_*^2 \bar{\theta}}{\gamma g [(1 + A)\, h - BkL]} \right\} \frac{\mathrm{d}h}{\mathrm{d}t} = \frac{(\overline{w'\theta'})_s}{\gamma} \tag{2b}$$

however no significant differences with eq. (2*a*) have been found.

Equations (2) refer to the convective boundary layer only. To get the evaluation of h continuous over the full range of atmospheric conditions, during stable conditions the PBL height was prescribed according to the following expression [22]:

$$h = 0.4 \sqrt{\frac{u_* L}{f}}, \tag{2c}$$

where f is the Coriolis parameter.

In the other two methods, the profile of gradient Richardson number Ri is considered and the height where Ri becomes greater than a critical value Ri_c is chosen as the PBL depth h. When Ri increases beyond a small positive number, Ri_c, turbulence tends to be suppressed, so that this value is used to identify the stable inversion layer capping the ABL. In the former of these methods (PBL*h*2) the critical value is taken constant and equal to 1.3, following Maryon and Buckland [23]. In the latter case (PBL*h*3), the McNider and Pielke [24] procedure is adopted. They chose to make Ri_c, a weak function of the model grid spacing in the form,

$$\mathrm{Ri}_c = a \Delta z^b, \tag{3}$$

where Δz is the model grid spacing in centimetres, $a = 0.115$ and $b = 0.175$. According to McNider and Pielke [24], Ri_c approaches the theoretical value 0.25 for the fine

vertical grid resolution near the surface, while away from the surface, where grid resolution is lower, Ri_c approaches 1.0, consistent with their observations.

Finally, from the values of u_*, L and h, the convective velocity scale can be determined as follows: $w_* = u_*(-h/kL)^{1/3}$.

2'3. *Turbulence fields.* – In the second stage, when surface layer parameters and PBL height are known, one can compute the turbulence fields, represented by the standard deviations and the Lagrangian time scales of the wind fluctuation field, σ_u, σ_v, σ_w, T_u, T_v and T_w. In the present analysis we considered three parameterization schemes, TU1, TU2 and TU3, suggested by Hanna [12], Rodean [13] and McNider [15], respectively.

Hanna proposed

$$\sigma_u = \sigma_v = u_* \left[12 + \frac{1}{2} \frac{h}{2|L|} \right]^{1/3}, \tag{4a}$$

$$\begin{cases} \sigma_w = 0.96 w_* \left(3\frac{z}{h} - \frac{L}{h} \right)^{1/3}, & \frac{z}{h} < 0.03, \\ \sigma_w = w_* \min\left\{ 0.96\left(3\frac{z}{h} - \frac{L}{h} \right)^{1/3}, 0.763\left(\frac{z}{h} \right)^{0.175} \right\}, & 0.03 < \frac{z}{h} < 0.4, \\ \sigma_w = 0.722 w_* \left(1 - \frac{z}{h} \right)^{0.207}, & 0.4 < \frac{z}{h} < 0.96, \\ \sigma_w = 0.37 w_*, & 0.96 < \frac{z}{h} < 1, \end{cases} \tag{4b}$$

$$T_{Lu} = T_{Lv} = 0.15 \frac{h}{\sigma_u}, \tag{5a}$$

$$\begin{cases} T_{Lw} = 0.1 \frac{z}{\sigma_w} \frac{1}{0.55 + 0.38(z - z_0)/L}, & \text{for } \frac{z}{h} < 0.1 \text{ and } -\frac{z - z_0}{L} < 1, \\ T_{Lw} = 0.59 \frac{z}{\sigma_w}, & \text{for } \frac{z}{h} < 0.1 \text{ and } -\frac{z - z_0}{L} > 1, \\ T_{Lw} = 0.15 \frac{h}{\sigma_w} \left[1 - \exp\left(-\frac{5z}{h} \right) \right], & \text{for } \frac{z}{h} > 0.1, \end{cases} \tag{5b}$$

in the unstable case,

$$\sigma_u = 2 u_* \left(1 - \frac{z}{h} \right), \tag{6a}$$

$$\sigma_w = \sigma_v = 1.3 u_* \left(1 - \frac{z}{h} \right), \tag{6b}$$

$$T_{Lu} = 0.15 \frac{h}{\sigma_u} \left(\frac{z}{h} \right)^{0.5}, \tag{7a}$$

$$T_{Lv} = 0.07 \frac{h}{\sigma_v} \left(\frac{z}{h} \right)^{0.5}, \tag{7b}$$

$$T_{Lw} = 0.10 \frac{h}{\sigma_w} \left(\frac{z}{h} \right)^{0.8}, \tag{7c}$$

in the stable case, and

$$\sigma_u = 2u_* \exp\left[- \frac{3fz}{u_*} \right], \tag{8a}$$

$$\sigma_w = \sigma_v = 1.3u_* \exp\left[- \frac{2fz}{u_*} \right], \tag{8b}$$

$$T_{Lu} = T_{Lv} = T_{Lw} = \frac{0.5(z/\sigma_w)}{1 + 15(fz/u_*)} \tag{9}$$

in the neutral case.

Rodean proposed a parameterization for the vertical velocity variance that is continuous for all elevations ($z_0 < z < h$) within the turbulent boundary layer and the full range of atmospheric conditions from unstable to stable ($-\infty < 1/L < \infty$). For the vertical velocity variance he suggested

$$\left(\frac{\sigma_w}{u_*} \right)^2 = C_1 \left(1 - \frac{z}{h} \right)^{3/2} + C_2 \left[\left(\frac{z}{h} \right) \left(\frac{h}{-L} \right) \right]^{2/3} \left(1 - C_3 \frac{z}{h} \right)^n \tag{10a}$$

(where $C_1 = 1.6$, $C_2 = 0$ for $L > 0$ and $C_2 = 2.4$ for $L < 0$, $C_3 = 0.8$ and $n = 2$), for the horizontal velocity variances

$$\left(\frac{\sigma_u}{u_*} \right)^2 = \left(\frac{\sigma_v}{u_*} \right)^2 = C_9 \left(1 - \frac{z}{h} \right)^p + C_{10} \left(\frac{z}{-L} \right)^{2/3} \tag{10b}$$

(where $C_9 = 4.5$, $C_{10} = 0$ for $L > 0$ and $C_{10} = 0.6$ for $L < 0$, $p = 3/2$), and for the Lagrangian time scales

$$T_{Lu} = T_{Lv} = T_{Lw} = \frac{2\sigma_w^2}{C_0 \varepsilon}, \tag{11}$$

ε is the rate of dissipation of turbulent kinetic energy estimated as

$$\varepsilon = \frac{u_*^3}{kz} \left[1 + C_4 \left(\frac{z}{h} \right) \left(\frac{h}{-L} \right) \right] \left(1 - C_5 \frac{z}{h} \right)^m \tag{12a}$$

in stable atmosphere ($z/L \geqslant 0$), and as

$$\varepsilon = \frac{u_*^3}{kz}\left[1 + C_6\left(\frac{z}{h}\right)\left(\frac{h}{-L}\right)\right]\left(1 - C_5\frac{z}{h}\right)^m + C_7\frac{h}{-L} \tag{12b}$$

in unstable atmosphere ($z/L < 0$), where $C_4 = 3.7$, $C_5 = 0.85$, $C_6 = 0.75$, $C_7 = 0.3$ and $m = 3/2$.

In his formulation, McNider deduced σ_u, σ_v and σ_w from the mesoscale variables and PBL parameterization in the following forms.

Under unstable conditions ($z/L \leqslant 0$):

$$\sigma_u = \sigma_v = u_*\left(12 + 0.5\frac{h}{|L|}\right)^{1/3}, \tag{13a}$$

$$\sigma_w = \left(1 - \frac{z_G}{H_T}\right)\sigma_{w*} = \left(1 - \frac{z_G}{H_T}\right)\frac{K_m}{A\lambda_m}, \tag{13b}$$

z_G and H_T being the height of topography and computation domain respectively; and under stable conditions ($z/L > 0$):

$$\sigma_u = \sigma_v = 2.3u_*, \tag{14a}$$

$$\sigma_w = 1.21\left(1 - \frac{z_G}{H_T}\right)\left(\frac{\mathrm{Ri_c} - \mathrm{Ri}}{\mathrm{Ri_c}}\right)^{0.58}\left[\left(\frac{\partial\overline{u}}{\partial z}\right)^2 + \left(\frac{\partial\overline{v}}{\partial z}\right)^2\right]^{1/2}, \tag{14b}$$

where: $\mathrm{Ri_c}$ is the critical Richardson number defined in eq. (3); K_m is the diffusion coefficient for momentum; A is a coefficient defined as

$$A = 0.31\left(1 - 3\frac{z}{L}\right)^{-1/3}\left(1 - 15\frac{z}{L}\right)^{1/4}\left(0.55 + 0.38\frac{z}{L}\right), \quad \text{for } \left|\frac{z}{L}\right| \leqslant 1,$$

$$A = 0.05\left(1 - 3\frac{z}{L}\right)^{-1/3}\left(1 - 15\frac{z}{L}\right)^{1/4}, \quad \text{for } 0.1\left|\frac{h}{L}\right| > \left|\frac{z}{L}\right| > 1,$$

$$A = 0.06, \quad \text{for } \left|\frac{z}{L}\right| \geqslant 0.1\left|\frac{h}{L}\right|.$$

Lagrangian time scales are determined from the scale of turbulence as evaluated from the turbulent spectra:

$$T_{L_i} = 0.2\frac{\beta_i\lambda_{m_i}}{\overline{U}} \tag{15}$$

in which $i = u, v, w$ and β is the ratio of Lagrangian to Eulerian time scale:

$$\beta_i = 0.6\frac{\overline{U}}{\sigma_i}$$

with $\overline{U} = (u^2 + v^2 + w^2)^{1/2}$ and the restriction $\beta_i \leqslant 10$, while the wavelengths of the maximum in the vertical and horizontal velocity spectra are estimated by

unstable case ($z/L \leqslant 0$):

$$\lambda_{mu} = \lambda_{mv} = 1.5h\,,$$

$$\lambda_{mw} = \frac{z}{0.55 + 0.38(z/L)}\,, \qquad \text{for } 0 \leqslant z \leqslant |L|\,,$$

$$\lambda_{mw} = 5.9z\,, \qquad \text{for } L < z \leqslant 0.1h\,,$$

$$\lambda_{mw} = 1.8h\left[1 - \exp\left[-4\,\frac{z}{h}\right] - 0.0003\exp\left[8\,\frac{z}{h}\right]\right], \qquad \text{for } 0.1h < z < h\,,$$

stable case ($z/L > 0$):

$$\lambda_{mu} = \lambda_{mv} = 0.7h\left(\frac{z}{h}\right)^{1/2},$$

$$\lambda_{mw} = z \text{ limited by } \lambda_{mw} \leqslant 2.91\,.$$

So far the analysis is limited to the mixing layer. However, SPRAY may need estimations of turbulent quantities above the PBL (in the residual layer) to perform simulations of nocturnal dispersion. In this layer Lagrangian time scales are kept constant to their value at the PBL height. Wind standard deviations are set equal to the square root of the ratio between the diffusion coefficients and the Lagrangian time scales.

Finally it is worth pointing out that the profiles of skewness of vertical velocity fluctuations (not reported here), which are also input to SPRAY under convectively unstable conditions, may be estimated by appropriate relationships (see, for instance, papers [13, 25, 26]).

3. – TRANSALP 1990 **campaign**

The data set used to test and compare the different parameterizations was gathered in the TRANSALP II campaign [16], which took place in the Ticino river valley (South Switzerland) on September 29th, 1990. TRANSALP experiments [27] were designed to study the transport of atmospheric trace constituents over the Alpine barrier from the western Po Valley (Italy) to the Swiss Plateau and vice versa. They were part of TRACT, a sub-project of EUROTRAC within the European initiative EUREKA [28]. TRANSALP II was carried out by an international collaboration among the Joint Research Centre of Ispra, Italy (JRC), Paul Scherrer Institut of Villigen, Switzerland (PSI), Osservatorio Meteorologico of Locarno Monti, Switzerland, ENEL/CRAM of Milan, Italy (ENEL) and C.N.R.-Istituto di Cosmogeofisica of Turin, Italy.

The situation of the day in which the tracer release took place was characterised by a mobile anticyclone moving from West Europe to East and the winds took a SW direction. In this day favourable conditions for the experiment prevailed, so that the tracer release could be considered successful.

In this work wind profile data collected by three Doppler Sodars are used: they were operated, respectively, by PSI (located in the proximity of the Gotthard Pass, 2100 m a.s.l), ENEL (Tecial, in the upper Leventina Valley, 1380 m a.s.l.) and JRC (near the Nufenen Pass, 2100 m a.s.l). The three Sodars measured the three wind velocity components and the standard deviations of vertical velocity fluctuations, with a

time step of 30 minutes. Data from radiosoundings performed by ENEL at Tecial giving pressure, temperature and humidity profiles from ground level to about 5000 m a.s.l. and from two sonic anemometers operated by JRC close to Giornico (in the Leventina valley, 360 m a.s.l, where the tracer was released), are also utilised.

4. – Input fields and RAMS configuration

The Regional Atmospheric Modeling System (RAMS) was developed at Colorado State University. As the present paper does not deal specifically with RAMS simulations, but just employs the fields resulting from a simulation performed by Martilli and Graziani [17], we refer the reader to the quoted paper and to Pielke's team papers (see, for instance, [9]). Here it suffices to recall a few facts, directly related to the present analysis.

RAMS is fundamentally a limited-area model, but may be configured, from the one hand, to cover an area as large as a planetary hemisphere for simulating mesoscale and large-scale atmospheric systems and, from the other side, because of its no lower limits in the domain size or to the mesh cell size of the model's grid, microscale phenomena can be simulated. Based on the 2-way grid interactive procedures of Clark and Farley [29], RAMS has the capability to nest from large-scale area to smaller scale. It has a non-hydrostatic option so that all meteorologically relevant spatial scales can be represented.

Two grids were nested in Martilli and Graziani [17] simulation. The coarse grid has an extension of 160 km E-W (from Valtellina to Monte Rosa) per 120 km S-N (from Como and Maggiore lakes to Quattro Cantoni lake), with a resolution of 4×4 km. The

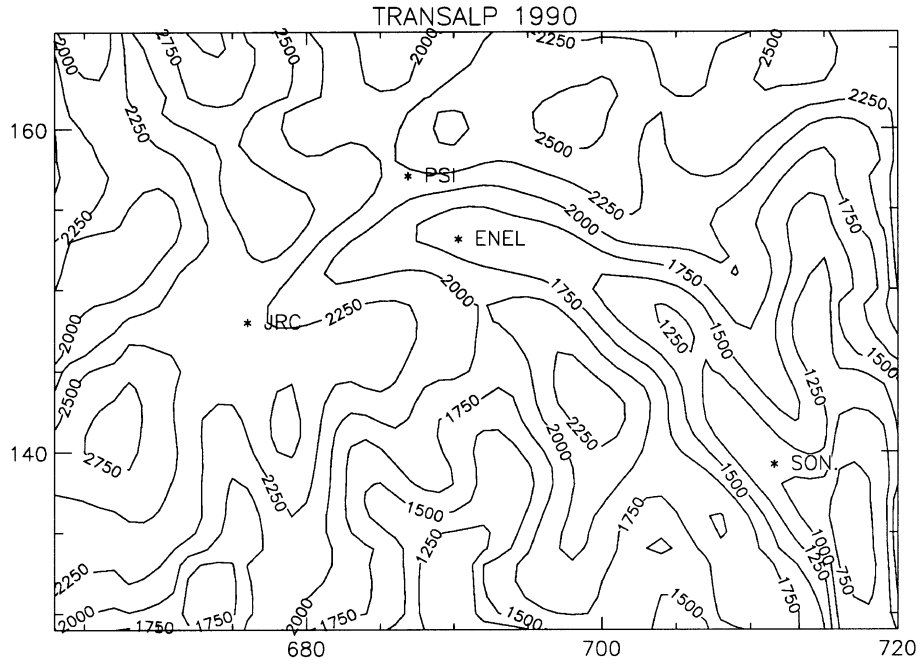

Fig. 1. – Topography isolines.

fine grid has an extension of 58 km E-W (from Blenio valley to Blinnernhorn ice) per 38 km S-N (from Biasca to Andermatt), with a space resolution of 1×1 km. Soil is taken uniform (sandy clay, tall grass) except in correspondence of the Dammastock and Blinnernhorn ices. There are 29 vertical levels, the first level is 35 m a.g. and the top level is 5500 m a.g. The integration time was 5 s. In the present work, the grid considered is the finer one, so that topography also is defined on it (see fig. 1). Roughness length was kept constant and equal to 0.1 m.

The simulation began at 18:00 LST on September 28 and ended at 6:00 on September 30. A sequence of 72 wind and temperature 3D fields was thus produced. RAMS configuration for the TRANSALP II simulation was characterised by the following options:

- non-hydrostatic,
- homogeneous initial conditions (Tecial sounding data),
- Klemp-Wilhelmson lateral conditions for velocity, null gradient at the boundary for the other variables,
- rigid-lid upper-boundary condition,
- Tremback-Kessler soil model lower-boundary condition,
- Smagorinsky turbulence parameterization,
- constant aerodynamic roughness,
- Arakawa type-C grid stagger,
- hybrid temporal integration method ("leapfrog" for the velocity components and the pressure, "forward" for the other variables).

As above anticipated, the following RAMS output fields are utilised throughout this paper: potential temperature, three wind components, vertical diffusion coefficients, registered every half an hour.

5. – Results of the intercomparison of turbulence schemes

Surface layer parameters, flow field from RAMS simulation and turbulence field from the parameterization schemes are compared with available observed data. Comparing actual data with model and parameterization scheme outputs must be carefully considered, since local and subgrid-scale effects cannot be resolved on the relatively coarse model grid spacing. On the contrary these features are accounted for by observation. For instance, fig. 2 shows the comparison between the heat flux h_0 measured by the two sonic anemometers, displaced about 220 meters apart and measuring at 8 m above the ground. Significant differences can be remarked on such a short distance. These can be explained by the different solar exposition of the two anemometers: they were placed in a valley section about 1 km wide and 1.5 km high. The western side of the valley was lighted first by the Sun, so that the instrument placed there measured higher heat flux values in the first part of the day. In the afternoon the opposite trend took place, whereas during night-time the two measurements are similar. Nocturnal fluctuations measured by both anemometers, appearing in the wind velocity records as well, are not clearly identifiable on the basis of the available information. They are likely to be caused by local circulations, induced by subgrid orographic features.

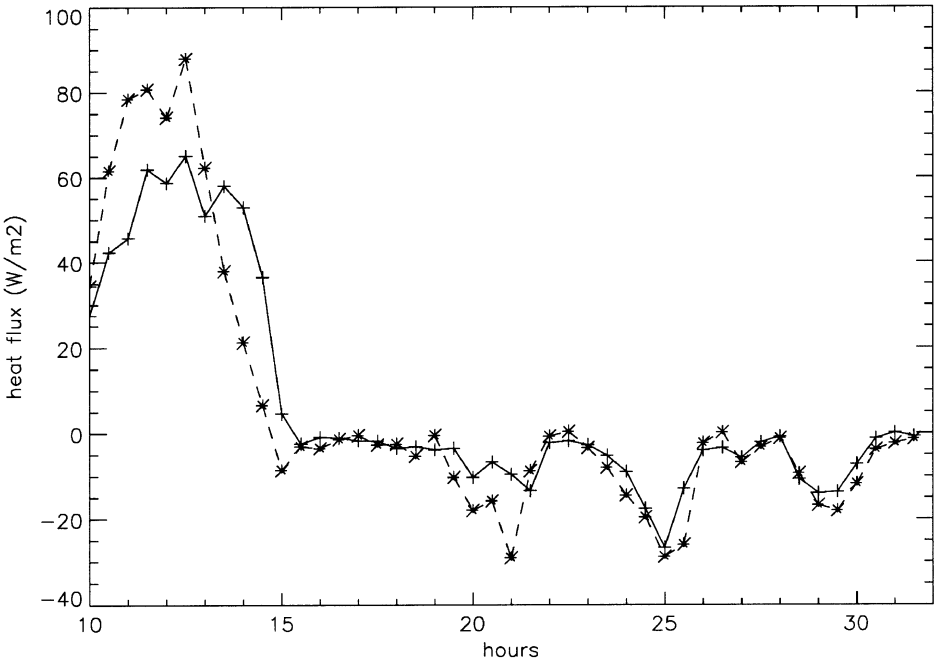

Fig. 2. – Comparison between heat fluxes measured by the two sonic anemometers. Dashed line corresponds to the anemometer on the western side of the valley, solid line to that on the eastern side.

To make the calculated data as homogeneous as possible with those observed, some interpolations have been performed. In the horizontal, the data of the four grid points nearest to the measuring locations have been interpolated with a bi-linear formula; in the vertical some common levels (corresponding to the Sodars' levels above ground) were chosen and all the data were linearly interpolated at those heights.

Some examples of the comparison between wind speed and direction measured by Sodars and produced by Martilli and Graziani [17] RAMS simulation are reported in figs. 3-6, for two heights: 60 and 300 metres above ground. As far as ENEL Sodar is concerned, at the lowest level the model simulation is able to reproduce data trend, but it overestimates speed values, in particular during the central hours of the day. Computed wind direction, which seems to be enough accurate, shows smaller fluctuations than observations. The agreement appears to be better at 300 m. On the contrary, in the case of PSI Sodar the agreement is better at 60 m than at 300 m. In this latter case, the model reproduces a daily fluctuation not detected by the instrument. This can be explained by PSI Sodar location: it was placed on the top of a mountain and not within a valley like the other two, so that it felt mainly the general circulation and was only slightly influenced by the diurnal cycle. As a consequence, it continuously measured high wind speed with little variations, while the model, taking into account the rather smoothness of its orography, is not capable to reproduce such an effect and, moreover, it solves the flux equations on a coarse grid. These considerations must be kept in mind while dealing with the intercomparison of surface layer and turbulence parameterization schemes.

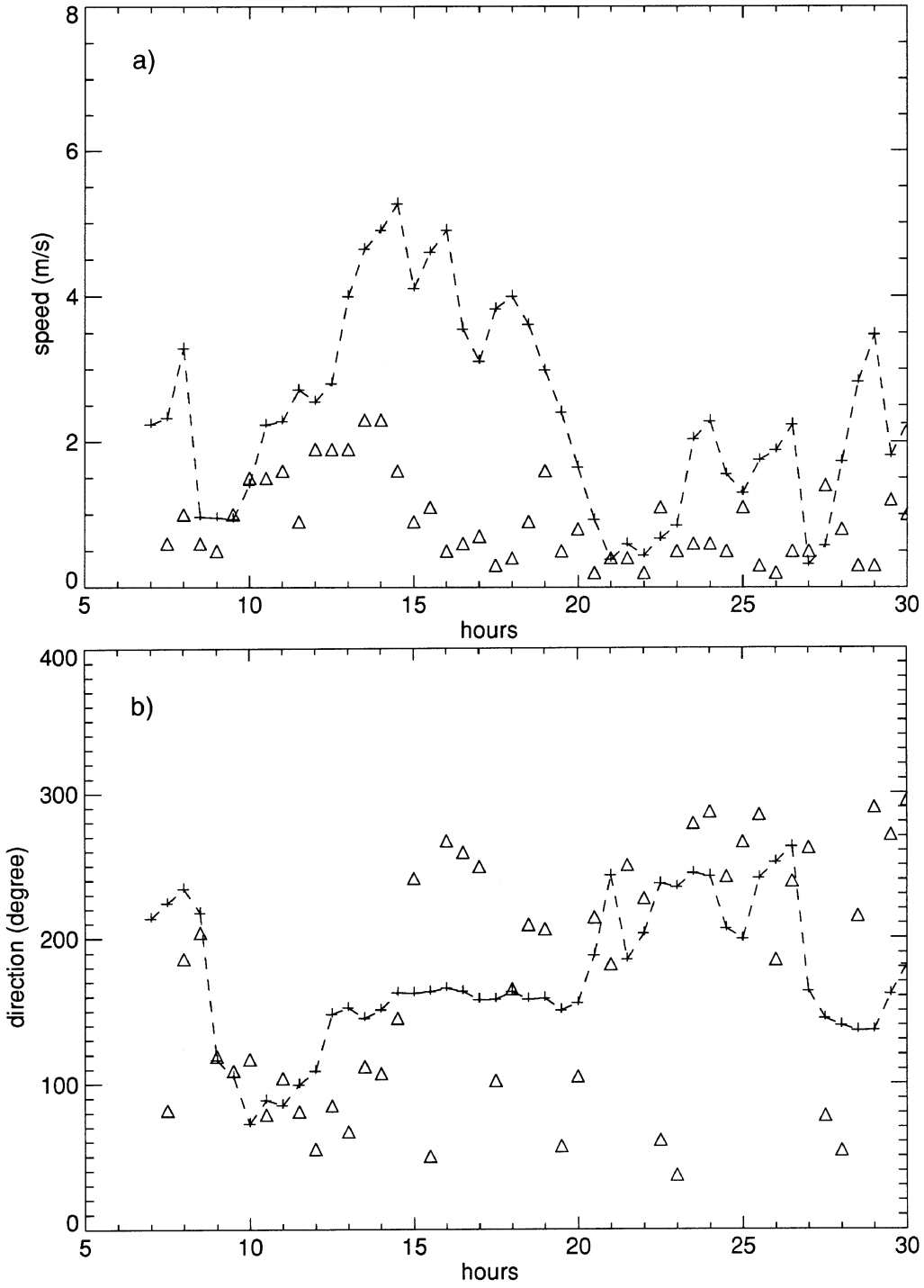

Fig. 3. – Comparison between wind speeds (a) and direction (b) calculated by RAMS (dashed line) and observed by ENEL Sodar at 60 m (triangles).

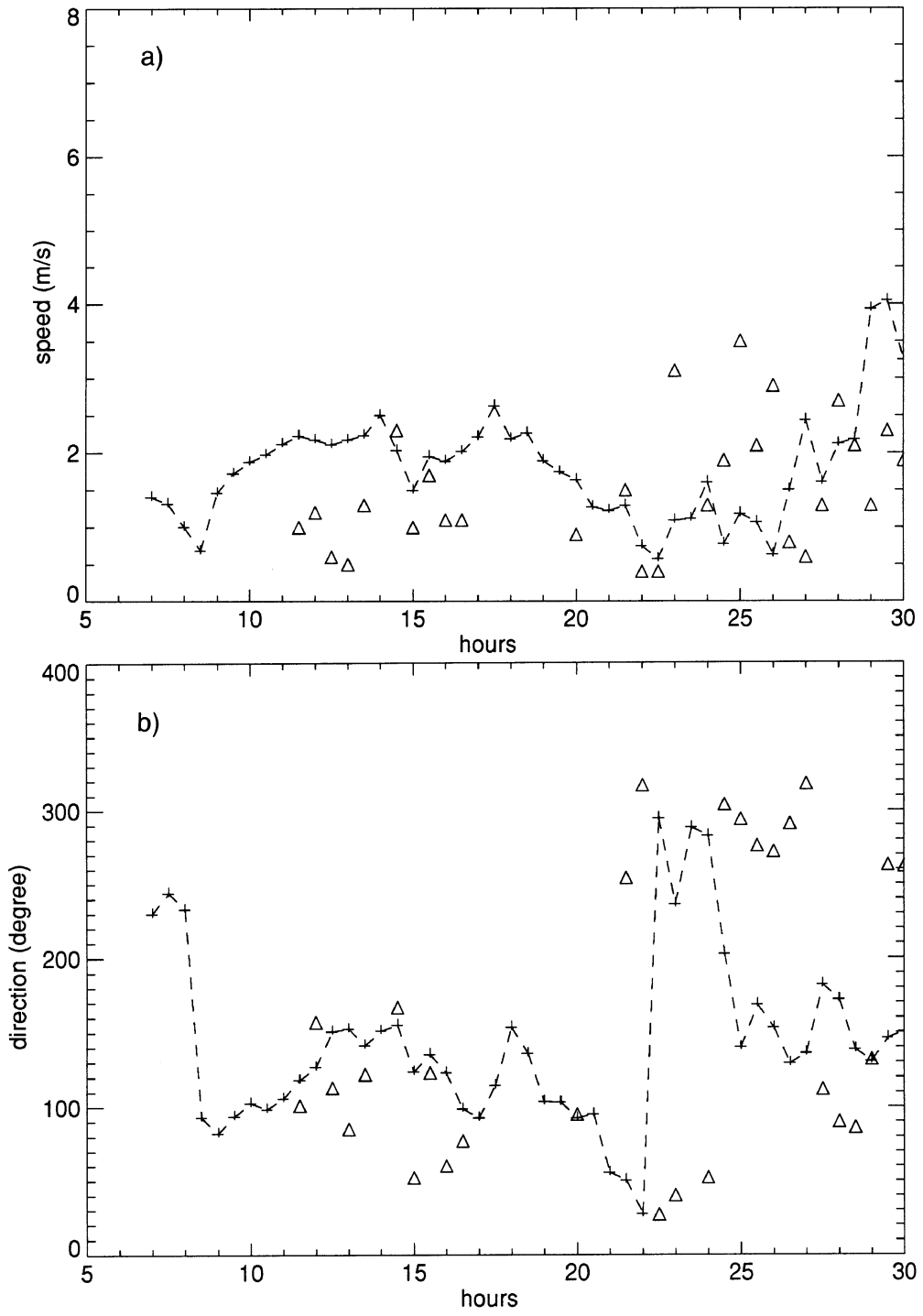

Fig. 4. – As in fig. 3 except at 300 m.

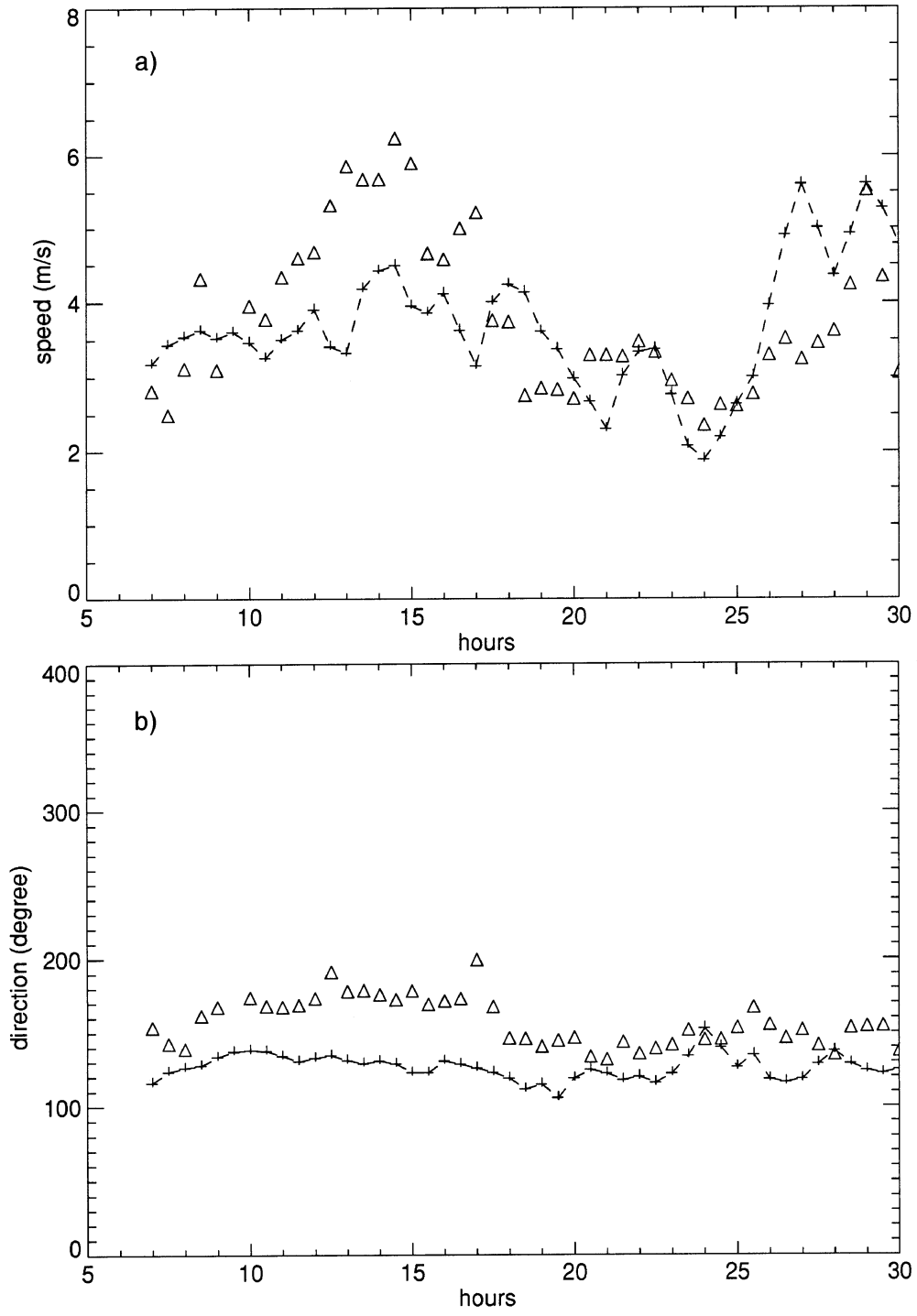

Fig. 5. – As in fig. 3 except for PSI Sodar.

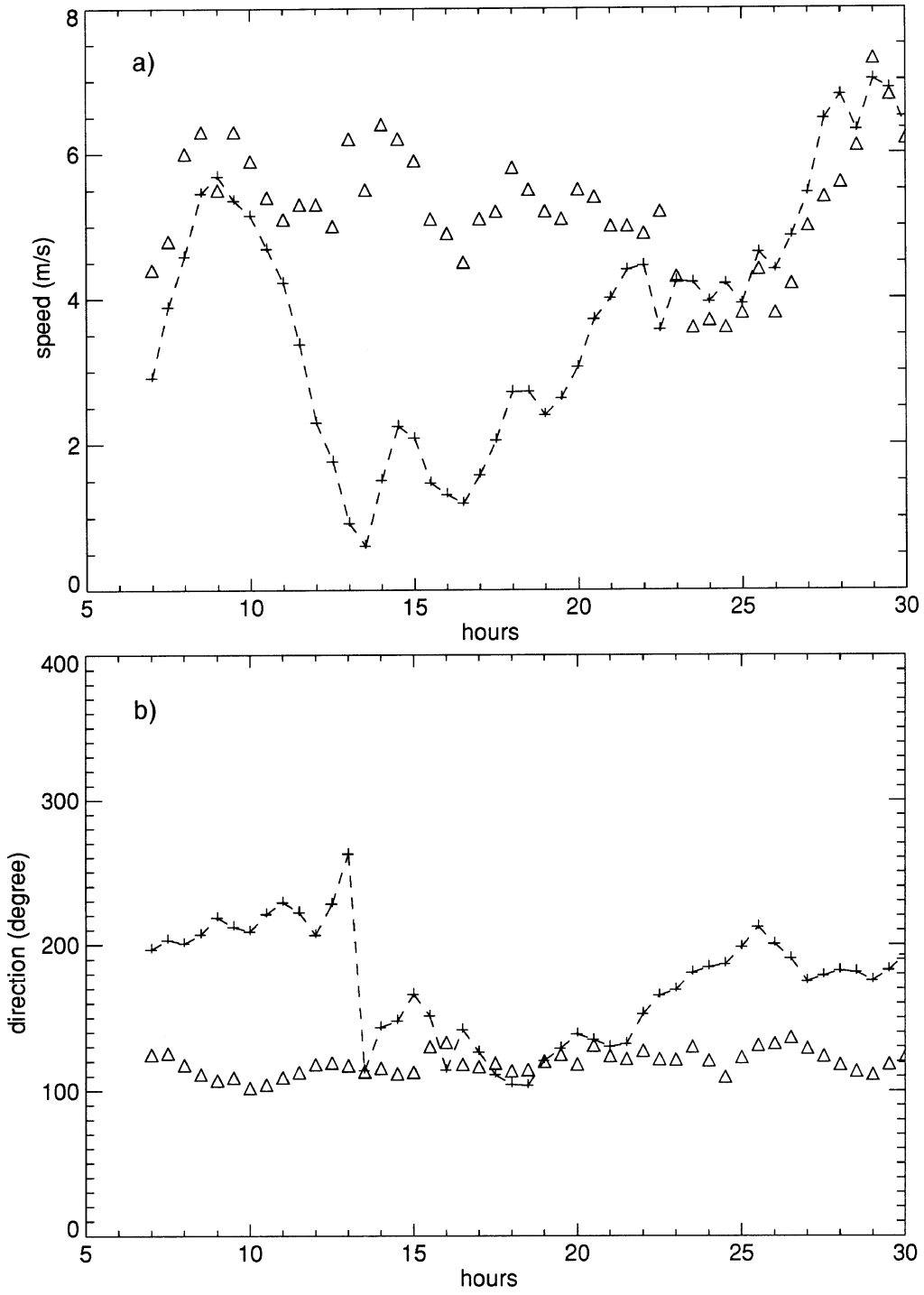

Fig. 6. – As in fig. 4 except for PSI Sodar.

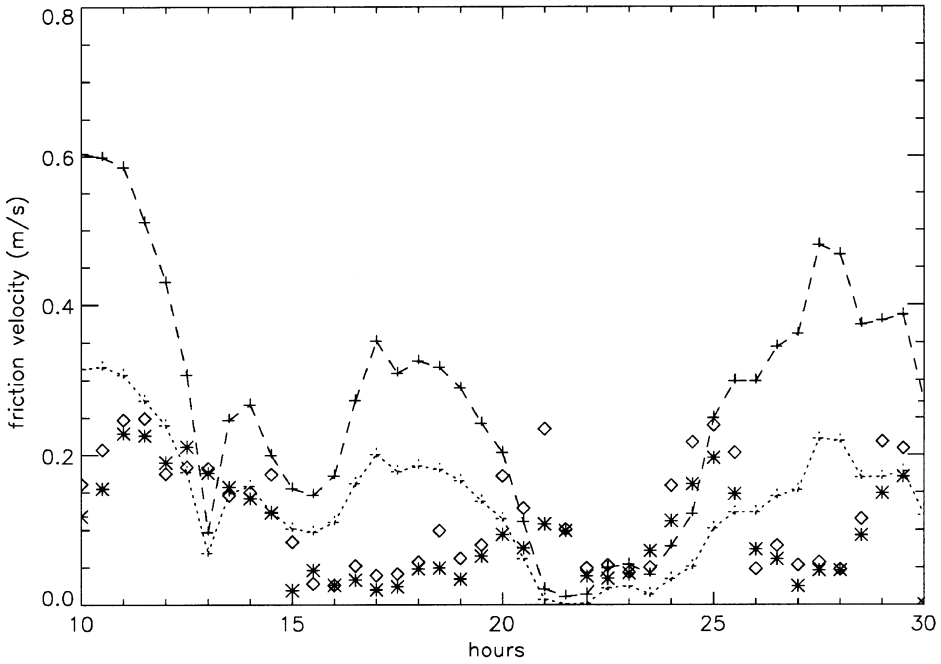

Fig. 7 – Comparison among friction velocity calculated with SL1 (dashed line) and SL2 parameterization (dotted line) and those measured by the two sonic anemometers (asterisks and diamonds).

Two different roughness values were tested: the first one, $z_0 = 0.1$ m, was considered the basic one because it was also used in the RAMS simulation and, moreover, was found by regression on the sonic anemometers wind speed records during neutral conditions; the second one, $z_0 = 1.5$ m, was estimated from the roughness table considering a typical mountain site covered by woods. The latter z_0 yielded the worst fitting of observed quantities. Therefore in the remnant of this work it was assumed that $z_0 = 0.1$ m.

5˙1. *Surface layer parameterization.* – In fig. 7 friction velocity courses, calculated by SL1 and SL2, are compared with those measured by the two sonic anemometers. SL1 curve overestimates measured data more than SL2. The trends of the two curves show a fair agreement, even in the case of the heat flux (fig. 8). In both graphs, the worst agreement between calculated and measured data occurs in the afternoon and during the night. In the first case the parameterization is probably not sensible to the transition from sunshine to shade, that instead is captured by the instruments, due to their position at the valley bottom. In the second case it cannot reproduce the fluctuations due to local phenomenon evidentiated by fig. 2.

A fair agreement between SL2 parameterization and measured data characterised Monin-Obukhov length, computed on the four grid points closest to the sonic anemometers' position (see fig. 9a)), while SL1 values over/underestimate data (fig. 9b)) in many cases (particularly during night-time).

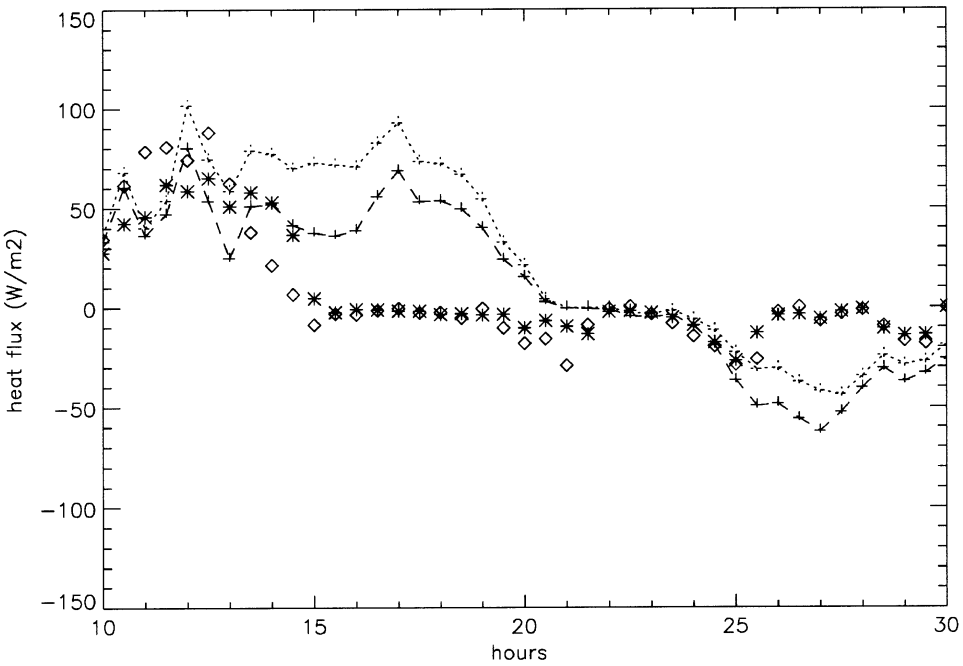

Fig. 8. – As in fig. 7 but for heat flux.

5˙2. PBL *height parameterization*. – To intercompare the three methods chosen for evaluating the PBL height temporal trend, the ENEL Sodar location (Tecial), in which some temperature profiles were available, is considered. Besides these methods, two other empirical evaluations of the mixing height are also considered: the first one derives from the consideration that the maximum in the σ_w profile during unstable conditions, in flat terrain, is found at about one third of the mixing height (see, for instance, [25, 30]); hence, inspecting the time sequence of the s_w profiles given by ENEL Sodar during the considered day, allows to estimate h; the second one is based on the RAMS diffusion coefficient K_z profiles, since K_z drops to very low values above h. However this last is only applicable during daytime because nocturnal K_z profiles generally attain low values at all levels without showing any appreciable discontinuity. These five different h values are shown in fig. 10 in which SL2 parameterization is used (solid, dotted and dashed lines correspond to PBLh1, PBLh2 and PBLh3; asterisks, triangles and crosses indicate h estimates by the temperature profiles, K_z profiles and σ_w profiles). While PBLh2 and PBLh3 yield an h value every half an hour independently of previous values, PBLh1 formulation has memory of the preceding ones, so its trend shows a very regular growth in time. On the contrary, the two curves evaluated from the gradient Richardson number profile (PBLh2 and PBLh3) exhibit large fluctuations. Their agreement with the estimated data is satisfactory. PBLh3 is always lower than PBLh2 and the two curves significantly differ during nighttime where the latter shows remarkable fluctuations not shown by PBLh3. This could mean that $\mathrm{Ri}_c = 1.3$ is not a correct choice for nighttime stable conditions. However no estimates of h were available after 5.30 p.m. and hence this point remains

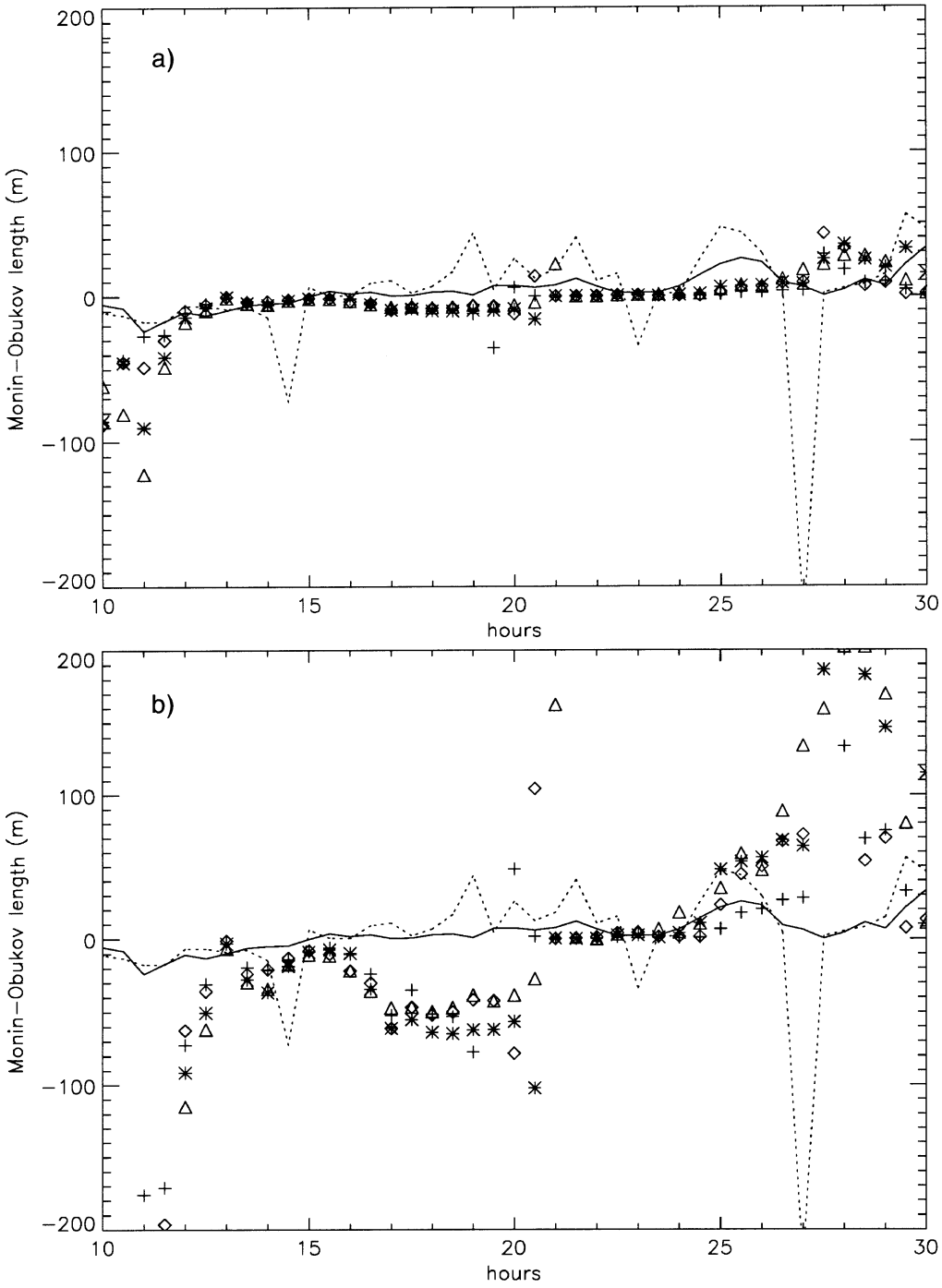

Fig. 9. – Comparison among Monin-Obukhov lengths measured by the sonic anemometers (solid and dotted lines) and those calculated with SL2 (a) and with SL1 (b) on the four grid points closest to them (triangles, crosses, asterisks and diamonds correspond to data at different points).

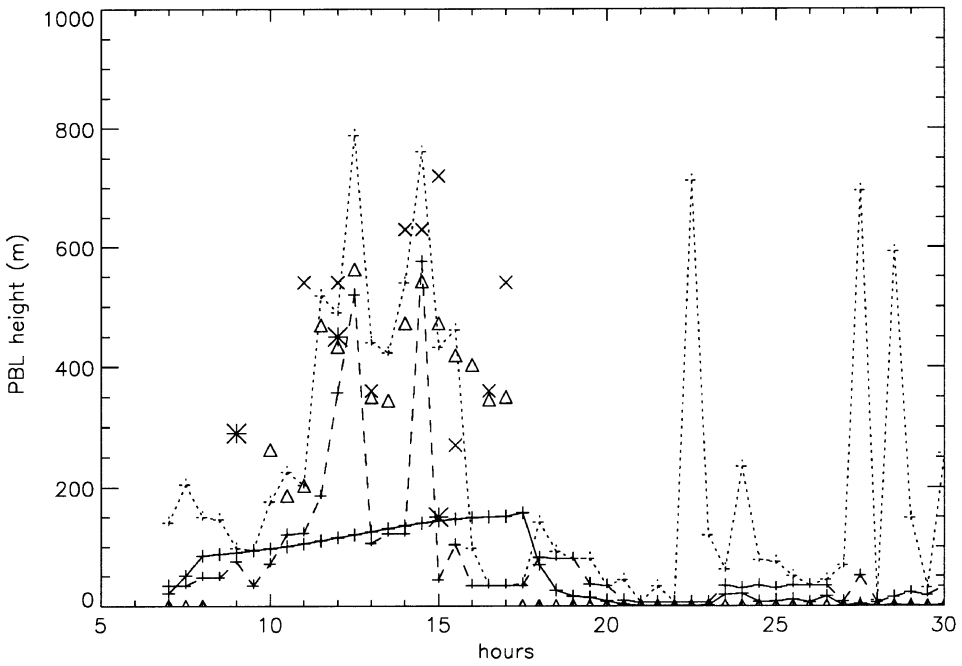

Fig. 10. – Comparison among mixing height evaluated with different methods using Louis surface layer parameters as input. Solid, dotted and dashed lines correspond to PBLh1, PBLh2 and PBLh3; asterisks, triangles and crosses indicate h estimates by the temperature profiles, K_z, profiles and σ_w profiles.

to be investigated. Repeating the calculations of fig. 10 with SL1 parameterization (not shown here) put in evidence that the main difference is a large difference between PBLh1 curves calculated using SL2 or SL1. Probably this is due to the way in which h depends on L (see eq. (2)). In fact these last values considerably differ in the two cases (see fig. 9a)-9b)).

5·3. *Wind velocity standard deviations.* – It is our opinion that Ri profile plays an important role in complex terrain: its calculation is sensitive to the turbulence inhomogeneities because it takes into account the velocity and temperature variations induced by orography. Therefore parameterizations based on Ri profile give to the relationships considered throughout this paper, which are strictly valid for flat terrain only, a certain degree of reliability in complex terrain. For this reason, in the present work, Ri is chosen as the basic quantity to calculate h.

Figure 11a) illustrates the comparisons among the σ_w measured by the two sonic anemometers and those calculated by TU1, TU2 and TU3 with surface layer parameters from SL1. The same comparison but with surface layer parameters estimated by SL2 is depicted in fig. 11b). It is to be pointed out that in these two drawings and in those which follow (except the last three) the PBL height considered is the one calculated by PBLh3 and the values of K_z needed for TU3 parameterization come from Louis parameterization.

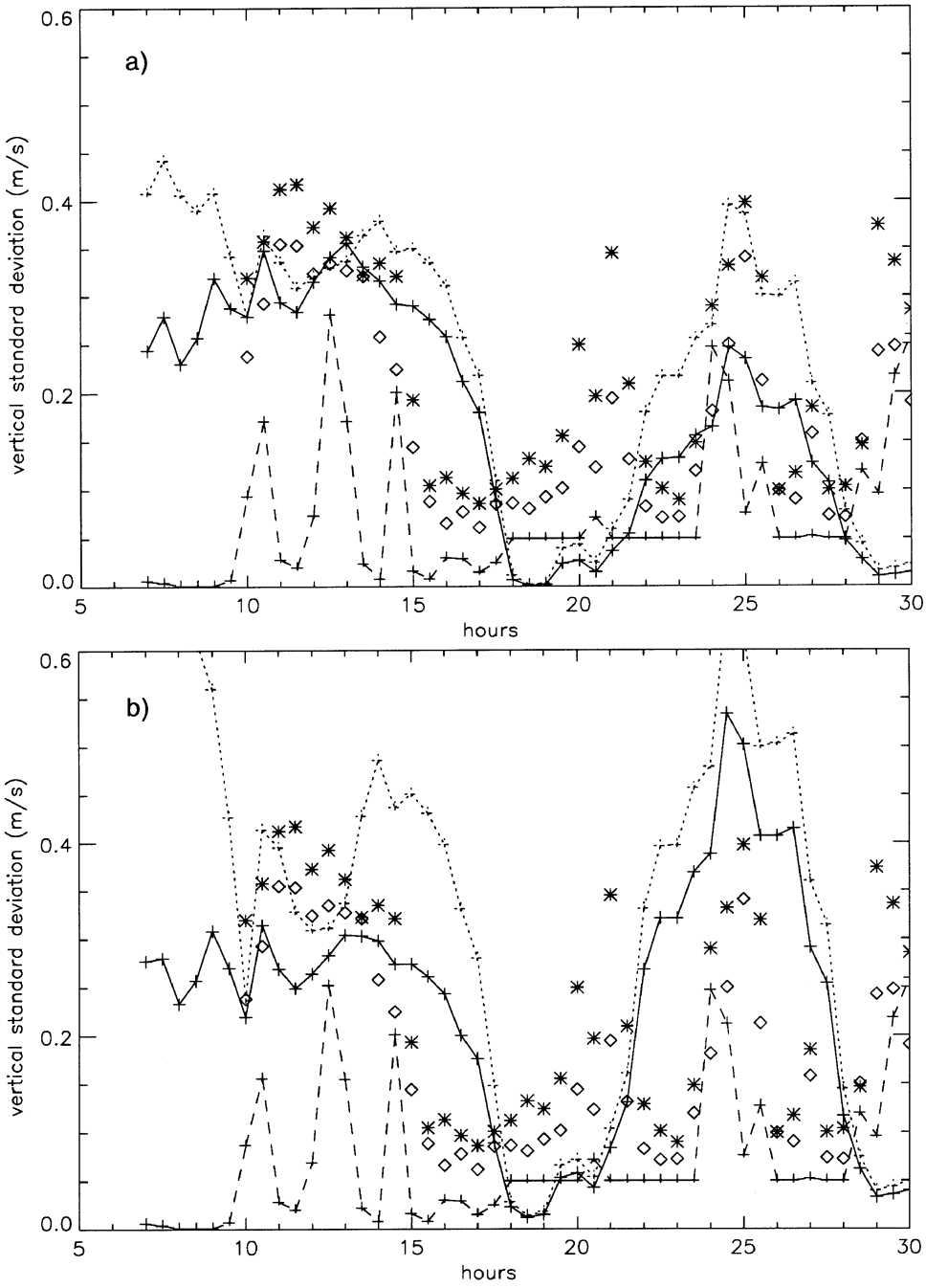

Fig. 11. – Comparison among vertical standard deviation calculated with three different methodologies following Hanna (solid line), Rodean (dotted line), McNider-Pielke (dashed line) and those measured by sonic anemometers (asterisks and diamonds); a) surface layer parameters by SL2, and b) with SL1.

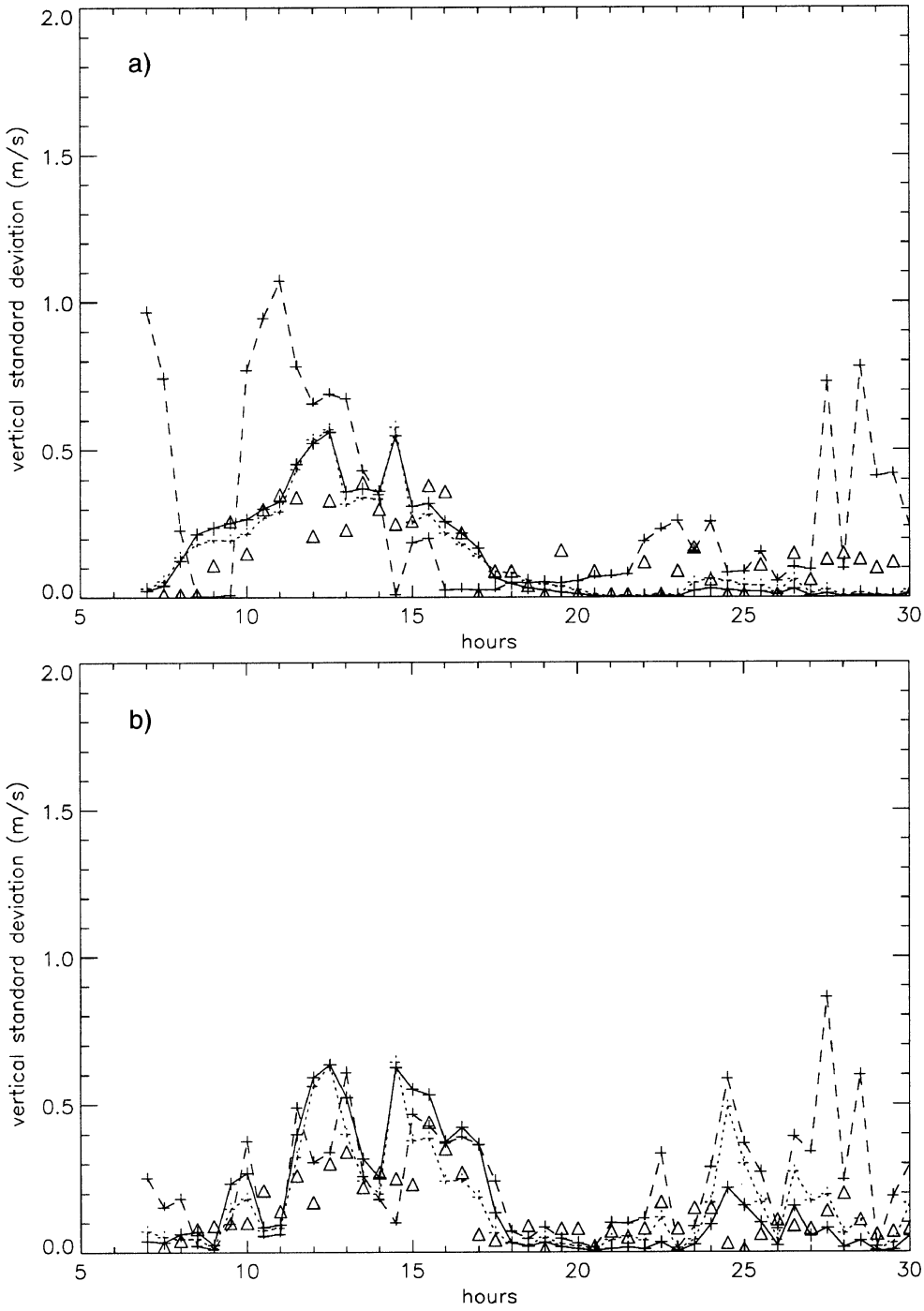

Fig. 12. – As in fig. 11 but with data measured by ENEL Sodar (triangles); a) $z = 60$ m and b) $z = 120$ m.

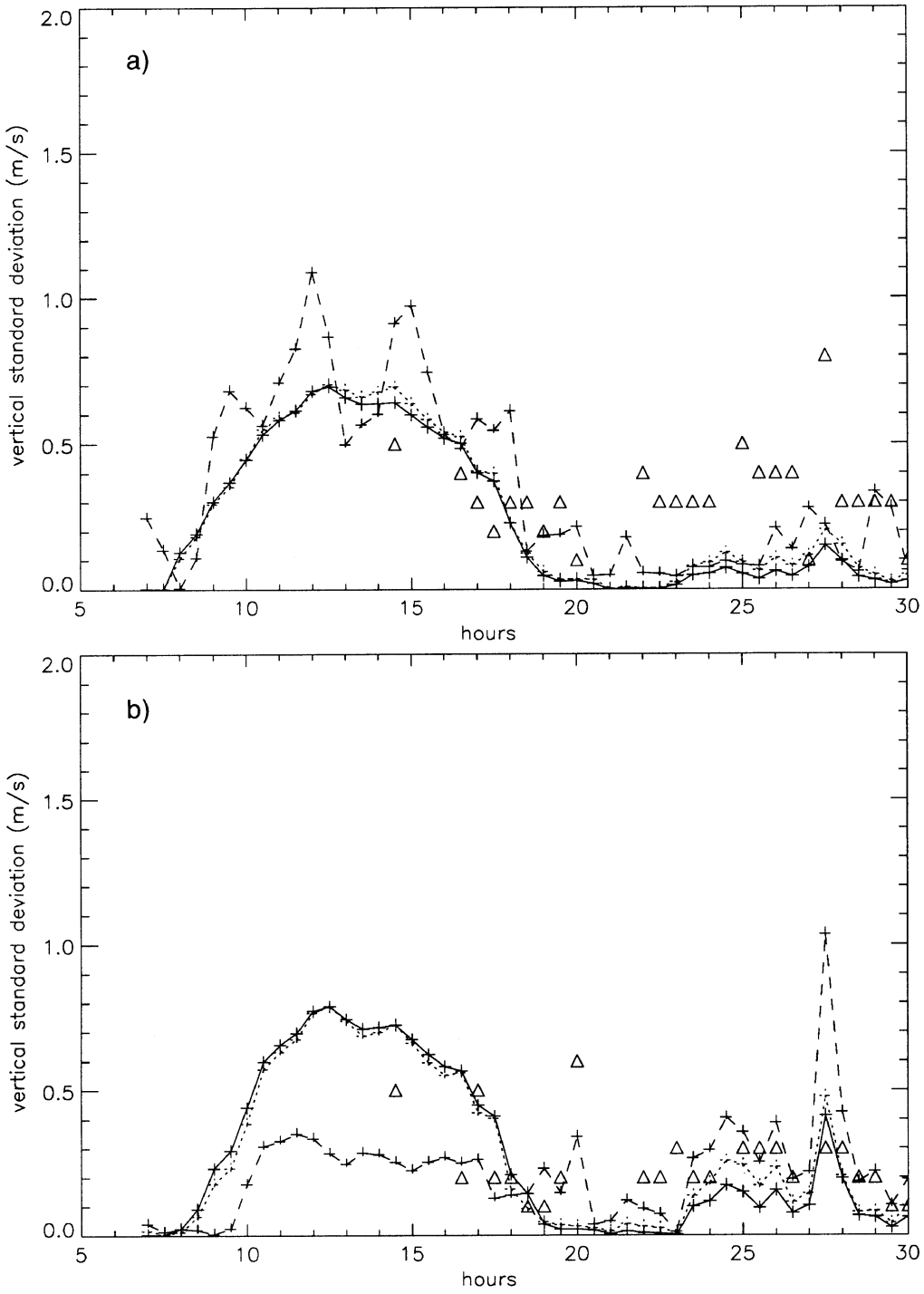

Fig. 13. – As in fig. 12, but for JRC Sodar.

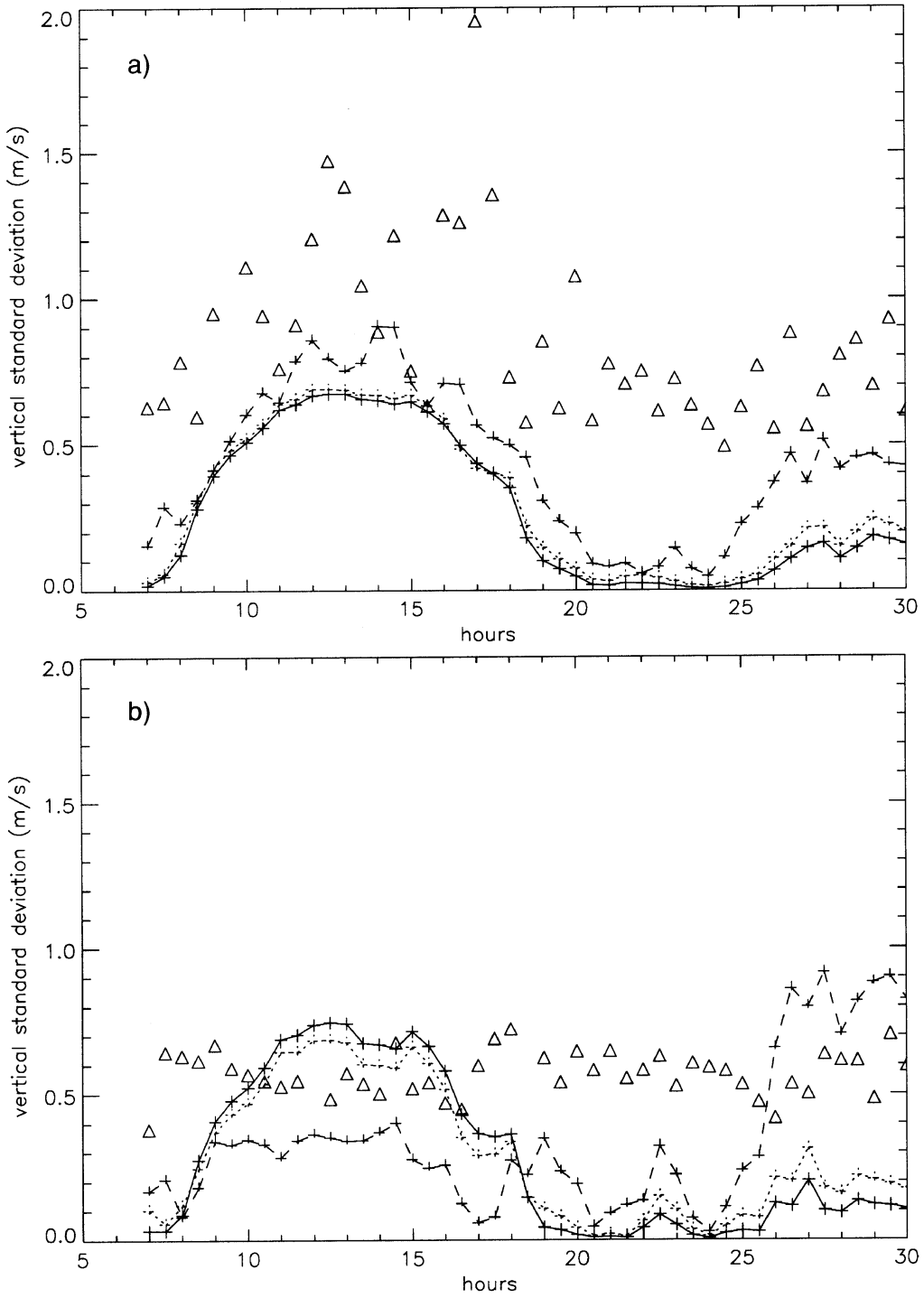

Fig. 14. – As in fig. 12, but for PSI Sodar.

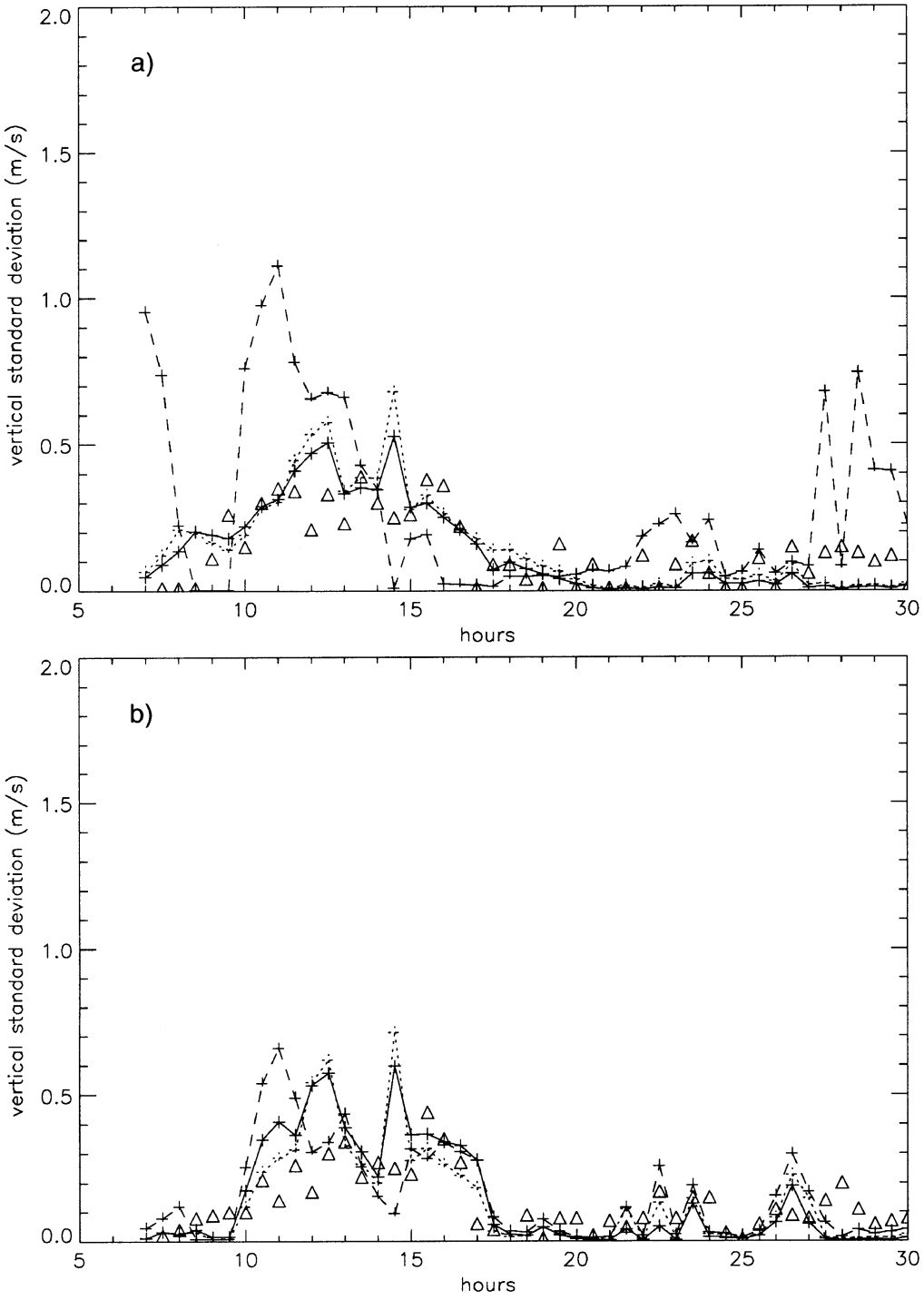

Fig. 15. – As in fig. 12, but with surface layer parameters by SL1.

An inspection of fig. 11 suggests that σ_w curve estimates based on SL2 parameterization are slightly preferable. Regarding the comparison among TU1, TU2 and TU3, the first two show a reasonable agreement with observed data (apart the period from 18.00 to 21.00); the second always gives estimate greater than the first one; the third one is the less sensible to the variation of surface layer parameters: this can be clarified looking at eq. (14*b*), in which there is no explicit dependence on them, apart in "A" expression.

Next figs. 12-15 show graphs which are similar to those reported in fig. 11 except they refer to the comparison with the three Sodar measurements. They refer to two different heights: 60 and 120 m. Since from the previous considerations it is concluded that SL2 appears to be preferable, figs. 12 to 14 are based on surface layer parameters derived from SL2. For comparative purposes, figs. 15, which are equivalent to figs. 12 (ENEL Sodar) illustrate what can be obtained with SL1. In general a very good agreement between TU1 and TU2 parameterizations is apparent, while TU3 shifts a bit more aside. Agreement with data is conditioned by the orography of the Sodar locations. For ENEL Sodar, the best agreement is at 60 m, while for JRC Sodar seems to be at 120 m. PSI Sodar graphs confirm what has been said above about wind velocity comparison, *i.e.* the parameterization produces a time-dependent behaviour not recorded by the instrument, placed on a peak; little variation is caught at the lowest level, 60 m.

Comparing figs. 12 and 15, it appears that the differences between the estimations of the two surface layer parameters have been smoothed by turbulence calculations, so that they have a smaller weight. The differences in fluctuations during the early morning hours at 120 and 300 m (these last not shown here) can be attributed to the fact that during such hours those heights are greater than the PBL depth. In these cases σ_w are evaluated with different diffusion coefficient values. Louis K_z profiles, more sensible to velocity and temperature profile fluctuations (see eq. (11)), are used in the first case (figs. 12), whereas the K_z ones from RAMS simulation output, which show a more regular growth with height, are utilised in the second case (figs. 15). However, K_z profiles from RAMS output seem less reliable than those from Louis parameterizations, as they have more a computational than a physical meaning (being grid spacing dependent).

6. – Conclusions

In this paper a parameterization scheme capable of producing reliable 3D turbulent quantities to be used as input of a Lagrangian particle diffusion model (SPRAY), on the basis of the outputs of a circulation model (RAMS), is presented. Various schemes (two for surface layer parameterization and three for PBL height and wind velocity standard deviation estimation) have been considered. Their different predicted values have been compared with each other and also compared to some observed values. These last were recorded during the second TRANSALP campaign [16]. The choice of the parametrization schemes was guided by the need of giving reliable estimates of the parameters of interest though maintaing a reasonable computational cost.

As surface layer parameters are concerned, the scheme suggested by Louis (SL2) appears to be preferable, especially with reference to the comparison between the two sonic anemometer records and calculations. Furthermore SL2 includes the calculation of K_z profiles that was demonstrated to be reliable. However it must be pointed out

that, even if SL1 and SL2 predictions differ considerably (compare figs. 11), this difference is not so great in the standard deviation results (compare figs. 12 and 15).

With regard to PBL height estimation it was found that the procedure suggested by Pielke-McNider, based on a variable critical R_i number, seems the more promising. For what concerns the turbulent quantities, only vertical standard deviation formulations could be tested, because typically Doppler Sodars do not give the horizontal standard deviations σ_u and σ_v, but the standard deviation of horizontal wind direction σ_θ and, moreover, no Lagrangian time scales or Skewness estimates were available. The results of this paper show that both TU1 and TU2 are reliable and more accurate than TU3.

Keeping in mind that actual data recorded in highly complex terrain have been compared to gridded estimated data, that orography in the computational domain was substantially smoothed, that utilised parameterizations were established for flat terrain, and, moreover, that input wind and temperature fields were obtained by a RAMS simulation output, the agreement between data observed and computed by the parameterization schemes, can be considered satisfactory. Obviously the results of this analysis cannot be regarded as general ones and must be carefully considered before being applied to different sites. This is also because the facts outlined above and the difficulty in getting measurements in complex terrain with the spatial and temporal resolution needed to make comparisons with model outputs, limit the possibility of going deeper into the details of the parameterizations and thus propose alterations to their formulation.

A remark concerns the fact that these turbulence parameterization schemes are defined within the mixed layer only: it can be important for dispersion modelling, especially when PBL height is very low (during night-time stable conditions, typically), to get turbulence fields in the residual layer too.

* * *

The authors wish to acknowledge the Joint Research Centre of Ispra, Italy, Paul Scherrer Institut of Villigen, Switzerland, Osservatorio Meteorologico of Locarno Monti, Switzerland and Centro Ricerche Ambiente e Materiali of ENEL, Milan (Italy) for the fruitful co-operation in organising and performing the TRANSALP 1990 campaign and for letting available to them their data gathered during that experiment.

REFERENCES

[1] ANFOSSI D., DESIATO F., TINARELLI G., BRUSASCA G., FERRERO E. and SACCHETTI D., to be published in *Atmos. Environ.*
[2] LAMPRECHT R. and BERLOWITZ D., to be published in *Atmos. Environ.*
[3] POULOS G. S. and BOSSERT J. E., *J. Appl. Meteorol.*, **34** (1995) 650.
[4] SEGAL M., PIELKE R. A., ARRITT R. W., MORAN M. D., YU C. H. and HENDERSON D., *Atmos. Environ.*, **22** (1988) 1319.
[5] TINARELLI G., ANFOSSI D., BRUSASCA G., FERRERO E., GIOSTRA U., MORSELLI M. G., MOUSSAFIR J., TAMPIERI F. and TROMBETTI F., *J. Appl. Meteorol.*, **33** (1994) 744.
[6] THOMSON D. J., *Q. J. R. Meteorol. Soc.*, **112** (1986) 511.
[7] YAMADA T., BUNKER S. and MOSS M., *J. Appl. Meteorol.*, **31** (1992) 565.

[8] BOYBEYI Z., RAMAN S. and ZANNETTI P., *Atmos. Environ.*, **29** (4), (Urban Atmosphere) (1995) 479.
[9] PIELKE R. A., COTTON W. R., WALKO R. L., TREMBACK C. J., LYONS W. A., GRASSO L. D., NICHOLLS M. E., MORAN M. D., WESLEY D. A., LEE T. J. and COPELAND J. H., *Meteorol. Atmos. Phys.*, **49** (1992) 69.
[10] SOZZI R., *Il Planetary Boundary Layer - Metodi per la stima della turbolenza*, Techn. Report SA-RI-06/94 (Servizi Territorio s.c.r.l., 1994).
[11] LOUIS J. F., *Boundary Layer Meteorol.*, **17** (1979) 187.
[12] HANNA S. R., *Applications in air pollution modeling*, in *Atmospheric Turbulence and Air Pollution Modelling*, edited by F. T. M. NIEUWSTADT and H. VAN DOP (Reidel, Dordrecht) 1982, Chapt. 7.
[13] RODEAN H. C., *Notes on the Langevin Model for Turbulent Diffusion of "Marked" Particles*, Techn. Report UCRL-ID-115869 (Lawrence Livermore National Laboratory, 1994).
[14] PIELKE R. A., ARRIT R. W., SEGAL M., MORAN M. D. and MC NIDER R. T., *Boundary Layer Meteorol.*, **41** (1987) 59.
[15] MC NIDER R. T., *Investigation of the impact of topographic circulations on the transport and dispersion of air pollutants*, Ph.D dissertation (U-M-I Dissertation Information Service, University of Virginia, 1981).
[16] AMBROSETTI P., ANFOSSI D., CIESLIK S., GRAZIANI G., GRIPPA G., LAMPRECHT R., MARZORATI A., STINGELE A. and ZIMMERMANN H., *The TRANSALP-90 Campaign. The second tracer release experiment in a sub-alpine valley*, EUR 15952 EN (Commission of the European Communities, 1994).
[17] MARTILLI A. and GRAZIANI G., to be published in *Atmos. Environ.*
[18] BUSINGER J. A., WYNGAARD J. C., IZUMI Y. and BRADLEY E. F., *J. Atmos. Sci.*, **28** (1971) 181.
[19] VAN ULDEN A. P. and HOLTSLAG A. A. M., *J. Clim. Appl. Meteorol.*, **24** (1985) 1196.
[20] GRYNING S. E. and BATCHVAROVA E., *Simple model of the daytime boundary layer height, Ninth Syposium on Turbulence and Diffusion* (American Meteorological Society) 1990, p. 379.
[21] BATCHVAROVA E. and GRYNING S. E., *Boundary Layer Meteorol.*, **56** (1991) 261.
[22] ZANNETTI P., *Air Pollution Modeling: Theories, Computational Methods and Available Software* (Van Nostrand Reinold) 1990.
[23] MARYON R. H. and BUCKLAND A. T., *Atmos. Environ.*, **28** (12) (1994) 2019.
[24] MC NIDER R. T. and PIELKE R. A., *J. Atmos. Sci.*, **38** (1981) 2198.
[25] DE BAAS H. F., VAN DOP H. and NIEUWSTADT F. T. M., *Q. J. R. Meteorol. Soc.*, **112** (1986) 165.
[26] CHIBA O., *J. Meteorol. Soc. Jpn.*, **56** (1978) 140.
[27] AMBROSETTI P., ANFOSSI D., CIESLIK S., GRAZIANI G., LAMPRECHT R., MARZORATI A., NODOP K., SANDRONI S., STINGELE A. and ZIMMERMAN H., to be published in *Atmos. Environ.*
[28] FIEDLER F., *Proposal of a Subproject "Transport of Air Pollutants Over Complex Terrain - TRACT"*, EUREKA ENVIRONMENTAL PROJECT (Karlsruhe, 1989).
[29] CLARK T. L. and FARLEY R. D., *J. Atmos. Sci.*, **41** (1984) 329.
[30] STULL R., *An Introduction to Boundary Layer Meteorology* (Kluwer Academic Publishers, Dordrecht) 1988.